

Local Connections to Specific Types of Layer 6 Neurons in the Rat Visual Cortex

Amir Zarrinpar^{1,2} and Edward M. Callaway^{1,2}

¹ Systems Neurobiology Laboratory, The Salk Institute for Biological Studies, La Jolla; and ² Neurosciences Program, University of California, San Diego, La Jolla, California

Submitted 19 September 2005; accepted in final form 28 November 2005

Zarrinpar, Amir and Edward M. Callaway. Local connections to specific types of layer 6 neurons in the rat visual cortex. *J Neurophysiol* 95: 1751–1761, 2006. First published November 30, 2005; doi:10.1152/jn.00974.2005. Because layer 6 of the cerebral cortex receives direct thalamic input and provides projections back to the thalamus, it is in a unique position to influence thalamocortical interactions. Different types of layer 6 pyramidal neurons provide output to different thalamic nuclei, and it is therefore of interest to understand the sources of functional input to these neurons. We studied the morphologies and local excitatory input to individual layer 6 neurons in rat visual cortex by combining intracellular labeling and recording with laser-scanning photostimulation. As in previous photostimulation studies, we found significant differences in the sources of local excitatory input to different cell types. Most notably, there were differences in local input to neurons that, based on analogy to barrel cortex, are likely to project only to the lateral geniculate nucleus of the thalamus versus those that are likely to also project to the lateral posterior nucleus. The more striking finding, however, was the paucity of superficial layer input to layer 6 neurons in the rat visual cortex, contrasting sharply with layer 6 neurons in the primate visual cortex. These observations provide insight into differences in function between cortical projections to first-order versus higher-order thalamic nuclei and also show that these circuits can be organized differently in different species.

INTRODUCTION

Layer 6 of the cerebral cortex contains a diverse population of neuron types. Understanding the functional connectivity of each cell type is important for revealing their roles in cortical processing. Pyramidal neurons in layer 6 of primary sensory cortices are the source of corticothalamic input to the primary thalamic relay nuclei. These cells are thought to be involved in feedback circuitry (Bourassa and Deschenes 1995; Zhang and Deschenes 1997, 1998). A subset of these corticothalamic layer 6 cells also targets the higher-order thalamic nuclei. Although the function of the higher-order thalamic nuclei is not well understood, one theory is that they mediate cortico-cortical interactions (Guillery and Sherman 2002).

Corticothalamic neurons of layer 6 have a sublaminar organization. In the rat cortex, cells in the upper half of layer 6 in the somatosensory and visual cortices project to their respective primary relay nuclei, the ventroposterior medial nucleus (VPM) and the lateral geniculate nucleus (LGN) (Bourassa and Deschenes 1995; Zhang and Deschenes 1997). Cells in the lower half of layer 6 of the somatosensory and visual cortex, project both to their respective higher-order thalamic nuclei

[the posterior thalamic nucleus (Po) and the lateral posterior nucleus (LP), respectively] and to their primary nuclei (Bourassa and Deschenes 1995; Zhang and Deschenes 1997). The sublaminar organization of these cells suggests that they could have distinct morphologies and intracortical connectivity.

Although in the rat visual cortex retrograde labeling has identified the sublaminar organization of corticothalamic projection neurons, there have been few studies that have analyzed the detailed morphologies of these cells, particularly comparing the cells in the upper and lower sublayers to find quantifiable differences. As a result, the intracortical circuitry of the layer 6 pyramidal cells is poorly understood, and the role that these cells may play in the visual cortical circuitry is still unknown. One model of cortical circuitry (Gilbert 1983; Gilbert and Wiesel 1983), based primarily on anatomical studies of the cat visual cortex, proposed that the main cortical input to layer 6 is from layer 5 with little input from superficial layers. However, more recent laser-scanning photostimulation studies of input to layer 6 pyramids in macaque visual cortex found that some types of layer 6 pyramidal cells receive strong superficial layer input (Briggs and Callaway 2001). These results bolstered cortical circuitry models that suggested deep layer neurons are important for providing feedback to superficial layers (Callaway 1998). It is unclear whether these differences, differences between species, or cell-type dependent diversity within each species.

This study has two objectives: to characterize the morphological diversity of neurons in layer 6 of the rat visual cortex and to distinguish quantitatively between cell subtypes and to characterize the laminar organization of functional excitatory inputs to these subtypes. By comparing our results to those found in other cortical regions, and other species, the role of layer 6 in visual cortical circuitry can be better understood.

METHODS

Slice preparation

Vibratome-cut coronal slices (400 μm) were prepared from the primary visual cortex of P25–P30 Long-Evans rats. Slices were cut in ice cold oxygenated (95% O₂–5% CO₂) artificial cerebral spinal fluid (ACSF) [which contained (in mM) 125 NaCl, 5 KCl, 26 NaHCO₃, 1.25 KH₂PO₄, 1.33 MgSO₄, 10 D-(+)-glucose, 3.15 CaCl₂, and 1

Address for reprint requests and other correspondence: E. M. Callaway, Systems Neurobiology Laboratory, The Salk Institute for Biological Studies, 10010 N. Torrey Pines Rd., La Jolla, CA 92037 (E-mail: callaway@salk.edu).

The costs of publication of this article were defrayed in part by the payment of page charges. The article must therefore be hereby marked “advertisement” in accordance with 18 U.S.C. Section 1734 solely to indicate this fact.

kynurenic acid] and then maintained submerged in the same ACSF solution heated to 35–37°C.

Photostimulation and input maps

We used an infrared Olympus DIC microscope with a $\times 40$, 0.8 NA water-immersion lens to visualize and target layer 6 neurons for whole cell recordings in living brain slices. Glass microelectrodes (6–10 M Ω resistance) filled with a potassium-gluconate-based intracellular solution (in mM, 130 K-gluconate, 10 HEPES, 2 MgCl₂, 10 EGTA, 0.5 CaCl₂, and 2.54 Na₂ATP) contained 0.5–1% biocytin for cell labeling.

Local stimulation of presynaptic input neurons by light-evoked conversion of ‘caged’ glutamate to glutamate (“photostimulation”) was used to map laminar sources of functional connections onto individual recorded neurons (Briggs and Callaway 2001, 2005; Callaway and Katz 1993; Katz and Dalva 1994; Sawatari and Callaway 1996, 2000; Yoshimura et al. 2005). Brain slices were bathed in oxygenated ACSF (without kynurenic acid) containing 100–125 μ M “caged” glutamate [γ -(α -carboxy-2-nitrobenzyl) ester, trifluoroacetate, L-glutamic acid –“CNB-glutamate”; Molecular Probes, Eugene, OR] at room temperature. Ultraviolet light (10-ms flash from an argon-ion laser) was focused to photostimulate a small discrete spot in the plane of the brain slice through the $\times 40$ microscope objective positioned above the slice. Whole cell voltage-clamp recordings (–65 mV) were made from a single layer 6 postsynaptic neuron, and inward excitatory postsynaptic currents (EPSCs) resulting from photostimulation of presynaptic neurons were measured.

To map the locations of input to a single cell, ~ 500 sites were stimulated sequentially in a pseudo-random pattern that covered all cortical layers. Stimulation sites were located throughout a rectangular area surrounding the recorded neuron, typically extending ~ 200 μ m laterally on either side of the cell and vertically from the white matter to layer 1. After each photostimulation event, voltage-clamp records were made for each stimulation trial to detect EPSCs. In addition, photostimulation trials were interleaved with control trials (no stimulation) to obtain spontaneous EPSCs (sEPSCs). After completion of photostimulation and recordings from a cell, the laser was used to burn alignment sites (< 10 μ m) into the slice so that x - y photostimulation coordinates could be assigned to their corresponding positions in the tissue. Lamina borders were determined using both cytochrome oxidase stain and thionin/Nissl stain.

The spatial resolution of this technique allows mapping of laminar-specific excitatory input in rat visual cortex. We supplemented previously published measures (Dantzker and Callaway 2000; Yoshimura et al. 2005) with a series of experiments to assess the spatial resolution of the laser-scanning photostimulation with our given parameters. This was also to ensure that the spatial resolution of cells did not differ between layers. Loose-patch extracellular recordings were made of cells throughout the cortical column (3–5 cells in each layer). We recorded the frequency of action potentials after a photostimulation event and found that our results matched previously published experiments; cells fired action potentials when focal uncaging occurred within ~ 50 μ m from cell soma (see Dantzker and Callaway 2000; Yoshimura et al. 2005).

Morphological analysis

After photostimulation, slices were fixed with 4% paraformaldehyde in 0.1 M PBS for 12–24 h, then submerged in 30% sucrose in PBS. Then the slices were resectioned at 80 μ m, and stained for cytochrome oxidase and biocytin to reveal alignment sites, laminar borders, and neuronal morphology using methods previously described (Fig. 1A) (see Yabuta and Callaway 1998a,b). Nissl stain of the visual cortex revealed that layer 6 can be divided into two parts. The upper part (usually called layer 6 or layer 6A), which is ~ 350 μ m thick, is separated from the white matter by a narrow, light band of oval-shaped cells (usually called layer 6B) that is no thicker than 100

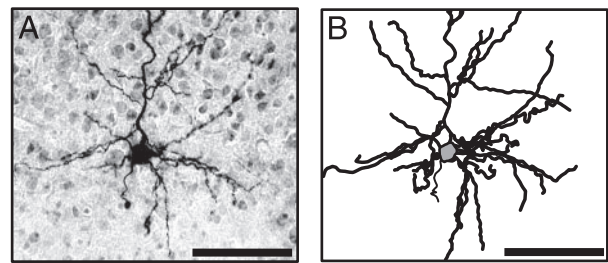


FIG. 1. A: cytochrome oxidase and thionin-stained section containing a biocytin-labeled layer 6 pyramidal neuron. B: neuroLucida reconstruction of cell in A. Dendrites are in dark black lines, soma is gray, and axon is thin line. Scale bars are 200 μ m.

μ m. Furthermore layer 6A could be easily separated from layer 5B with a combination of cytochrome oxidase and Nissl stains. Layer 6A was darker than layer 5B with cytochrome oxidase and more densely populated than layer 5B with Nissl stain. We will only discuss cells located in layer 6A in this study and will refer to it as layer 6. Because the thickness of layer 6A varies from slice to slice and animal to animal, we normalized the depths of the cells within this layer by dividing the distance of the soma from the layer 6A/6B border to entire length of layer 6A.

After staining, labeled dendritic processes were reconstructed using a $\times 40$ objective (oil immersion, 1.30 NA) and NeuroLucida, a computerized system (MicroBrightField, Williston, VT; see Figs. 1B and 2). After neuronal reconstructions were completed, sections were counterstained for thionin to visualize borders not well delineated with cytochrome oxidase stain alone. Each neuronal reconstruction, showing the morphology of the cell, the laminar borders, and the alignment sites, were aligned with the coordinate map of stimulation sites using Adobe Illustrator (Adobe Systems, San Jose, CA). Using custom software made with Matlab (The MathWorks, Natick, MA), we measured the length of basal and apical dendrites as well as the numbers of their respective branches and terminations within each layer. Cells with poor biocytin labeling, such that their anatomical type could not be determined, were excluded from the study. Some cells were well-labeled without collecting of photostimulation data and are included only for the anatomical studies. For nine of the cells, the soma was lost during resectioning. For these cells the depth of the soma within layer 6 was incalculable, but, because the cut occurred near the base of apical dendrite, enough of the apical dendrite structure remained to classify the cells based on their morphology.

Because we were concerned that cortical columns may be askew to the plane of the slice and hence may affect the number of evoked EPSCs from superficial layers, we took certain precautions to ensure that the circuitry to the apical dendrite was intact. First, we blocked the tissue during slicing to minimize the skewing of the apical dendrite and neuron column to the plane of the slice. Second, we eliminated any cells that had apical dendrites that were angled $> 30^\circ$ from the plane of the slice. Finally we did five control experiments, where we obtained simultaneous recordings from layer 5 and layer 6 pyramidal cells. Previous photostimulation experiments in layer 5 (Schubert et al. 2001) show that layer 5 pyramidal cells receive strong input from superficial layers, regardless of cell subtype. Likewise, in our control experiments we found that layer 5 pyramidal cells received strong superficial input, whereas concurrent measurements from layer 6 pyramidal cells within the same slice showed an absence or weakness of input from these layers (see Supplementary Fig. 1¹ and RESULTS). Finally, our data show that there is no relationship between a cell’s input and/or strength of input from superficial layers and its apical dendrite angle (in relation to the plane of slice; data not shown). Hence, it is unlikely that the angle of slice cutting prevented detection of connections from the superficial layers.

¹ The Supplementary Material for this article (a figure) is available online at <http://jn.physiology.org/cgi/content/full/00974.2005/DC1>.

Analysis of EPSCs

We analyzed EPSCs that occurred during the first 150 ms after photostimulation. This window was chosen because presynaptic neurons fired most of their APs during this time (see Dantzker and Callaway 2000; Yoshimura et al. 2005), indicating that shorter analysis windows would exclude photostimulation-evoked EPSCs. We distinguished direct effects of focal uncaging of glutamate on the recorded cell, which had a distinct shape (longer rise-time) and occurred immediately after glutamate uncaging (shorter latency; see, for example, Fig. 4A, trace 3) from EPSCs, and included only EPSCs in our analysis. After photostimulation, within $\sim 50 \mu\text{m}$ of the recorded cell, direct currents sometimes exceeded 100 pA and decayed over 100 ms, preventing EPSCs from being separately identified at these locations, and thus these sites were excluded from analysis. The amplitudes and numbers of EPSCs were measured for every stimulation site and for the no-stimulation controls using peak analysis software from Synaptosoft (Leonia, New Jersey) and other custom software. Each trial was assigned a value in picoampere, equal to the sum of the peak amplitudes of all detectable EPSCs. Stimulation sites were then assigned to their correct cortical layer, and EPSC amplitudes for all stimulation sites within a layer were pooled together using custom Matlab programs. Laminar groupings of EPSC sum of amplitudes were then compared with spontaneous EPSCs to identify statistically significant differences in EPSCs from a particular layer using Mann Whitney *U* tests. We also calculated the mean value of summed EPSC amplitudes for that layer as well as for control trials, measuring spontaneous EPSCs. To quantify the evoked input (EI) from a particular layer, the mean sum of amplitudes of spontaneous events was subtracted from the mean sum of amplitudes for each layer. The relative strength of excitatory input from each layer was calculated by dividing the EI for that layer by the sum of the EIs from all layers for that same cell. Cells were then grouped based on their morphological characteristics. In addition, if a cell did not receive significant input from a layer, the EI for that layer was set to 0 to avoid negative EI and EI percentages. Significant differences in layer-specific EI percentages between cell types were determined using Mann Whitney *U* Test.

To illustrate input patterns for individual cells, smoothed graphs of excitatory input were generated using custom Matlab programs (see Fig. 4 and Fig. 6). Values of the sum of amplitudes for each individual stimulation site were used to create these smoothed plots using linear interpolation. These plots illustrate estimated evoked activity measured in a given cell (mean sum of EPSC amplitudes for simulated trials minus mean sum of EPSC amplitudes for spontaneous trials) after stimulation at various locations. These plots are purely for illustration of the source of input; no part of the quantitative analyses was based on these linear interpolations.

RESULTS

Morphological results

We intracellularly labeled and reconstructed the morphologies of 89 layer 6 neurons in rat visual cortex. All cells were categorized into six different subtypes based on their dendritic morphology. Most of these subtypes have been described in Zhang and Deschenes (1997) single-cell labeling study of layer 6 in the rat somatosensory cortex, and we found that all our visual cortical cells had homologous morphologies to cells in somatosensory cortex.

Thirteen cells had aspiny dendrites, local pervasive axonal projections, and nonpyramidal somata (Fig. 2A) and were classified as inhibitory interneurons (13/89, 14.6%). These cells were found in the upper 2/3 of layer 6 (Fig. 3A, Table 1). The lack of these cells in the lower third is nearly significant ($P = 0.06$, Fisher exact test).

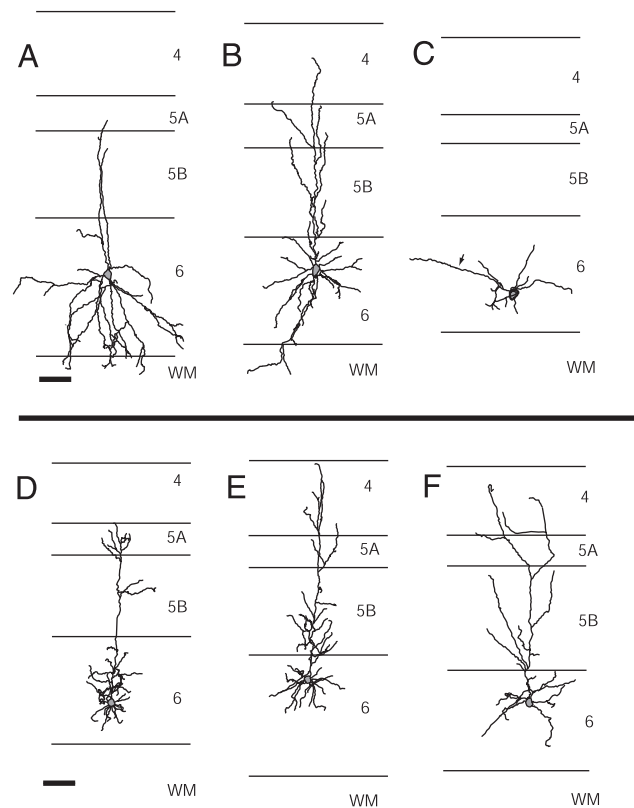


FIG. 2. NeuroLucida drawing of 6 different neuron subtypes differentiated by dendritic morphology in layer 6 of rat visual cortex. Dark lines, dendrites; gray, somata. Axons have been excluded from the drawings. *A*: inhibitory interneuron, identified by smooth, aspiny dendrites and nonpyramidal soma. *B*: bipolar excitatory cell, characterized by 2 large-diameter, vertically oriented spiny dendrites. One large-diameter dendrite projects toward the pia, whereas the other projects into the white matter. *C*: inverted pyramidal cells, characterized by pyramidal soma but a thick large-diameter dendrite (arrow) that did not project from the pial side of the soma. In this case, the thick large-diameter dendrite ran parallel to the pia. *D*: type I tufted pyramidal cell, characterized by an apical dendrite that had many perpendicular branches in layer 6, sparse perpendicular branches in layer 5B, and a tuft of dendritic branches in layer 5A, with none of the dendrites projecting into layer 4. Basal dendrites are contained within layer 6. *E*: type II tufted pyramidal cell, characterized by an apical dendrite with perpendicular branches in layer 5B and with one dendritic tuft that extends through 2 layers (layer 5A and layer 4). *F*: nontufted pyramidal cell, characterized by long angular branches from the apical dendrite, especially at the layer 5B/6 border. Apical dendrite does not end in a tuft. Both scale bars represent 200 μm .

The remaining neurons all had spiny dendrites suggesting that they were excitatory neurons. Most had a typical pyramidal morphology (see following text). However, nine cells had modified pyramidal morphologies described previously as bipolar excitatory (4/89 cells, 4.5%) or inverted pyramidal cells (5/89 cell, 5.6%) (Zhang and Deschenes 1997). Bipolar excitatory cells (Fig. 2B) were characterized by two large-diameter, vertically oriented, spiny dendrites. One of these dendrites projected toward the pial surface, whereas the other projected into the white matter. The large diameter basal dendrite in all cases was much thicker and longer than other basal dendrites, making these cells quite distinct from other pyramidal cells. Bipolar excitatory cells were found throughout the layer (Fig. 3A), and their counterparts in the rat somatosensory cortex had cortico-cortical projecting axons (Zhang and Deschenes 1997).

Inverted pyramidal cells (Fig. 2C) had a pyramidal-shaped soma, but the thick, large-diameter dendrite (the "apical"

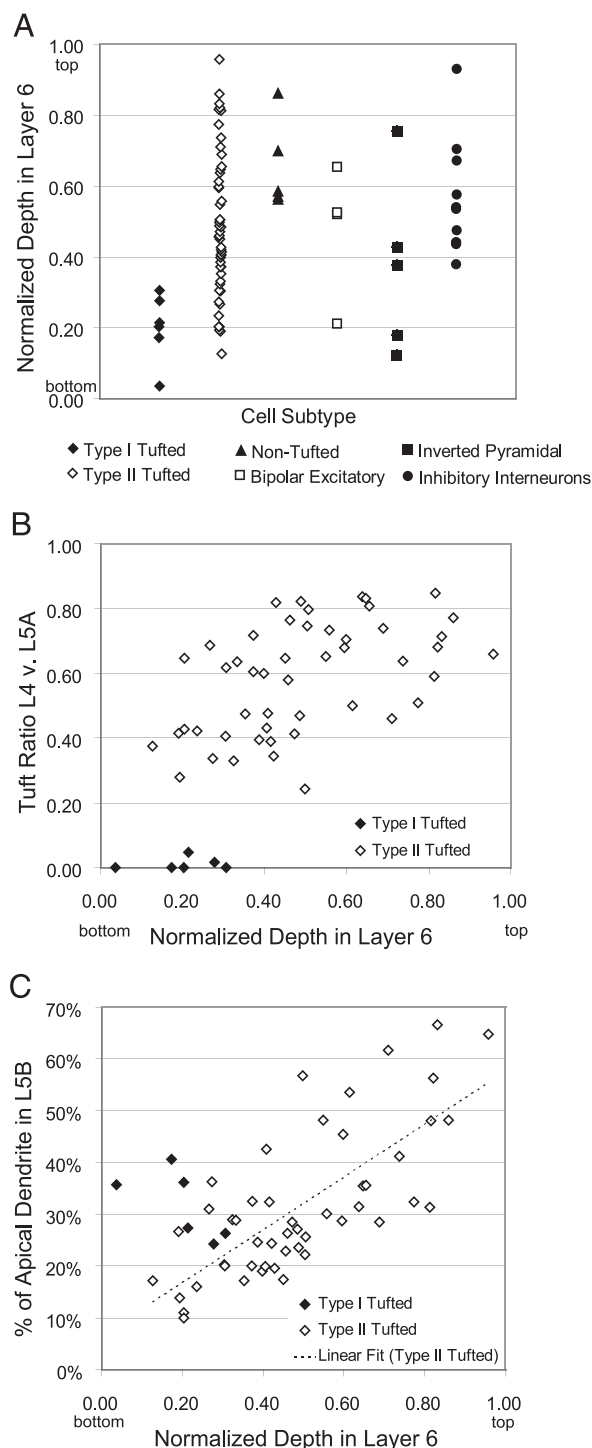


FIG. 3. *A*: distribution of cell subtypes within layer 6. The normalized depth within layer 6 is defined by the distance of soma from the layer 6A/6B border divided by total length of layer 6A. Type I tufted pyramidal cells are located in the lower third of layer 6A, whereas type II tufted pyramidal cells are found throughout the entire layer (see also Table 1). Non-tufted cells are found in the upper half of layer 6. All other types of cells are found throughout the layer. *B*: the relationship of normalized cell depth and tuft ratio. The tuft ratio is calculated by dividing the length of apical dendrite in layer 4 by the sum of the lengths in layer 4 and layer 5A. Type I and type II tufted pyramidal cells are clearly separated and not part of a continuum. *C*: relationship of normalized cell depth to the percentage of apical dendrite in layer 5B. Percentage of apical dendrite in layer 5B is determined by dividing the length of apical dendrite in layer 5B by total apical dendritic length. \cdots , fitted to type II tufted pyramidal neurons ($P < 0.001$). Type I tufted pyramidal neurons do not follow the same trend (see text).

TABLE 1. Distribution of cell somata within the depth of layer 6

	Lower Third	Middle Third	Upper Third	Total
Inhibitory interneurons	0 (0.00)	8 (18.6)	3 (18.8)	11
Bipolar excitatory	1 (4.8)	3 (7.0)	0 (0.00)	4
Inverted pyramidal	2 (9.5)	2 (4.6)	1 (6.2)	5
Non-tufted	0 (0.00)	3 (7.0)	2 (12.5)	5
Type I tufted	6 (28.6)	0 (0.00)	0 (0.00)	6
Type II tufted	12 (57.1)	27 (62.8)	10 (62.5)	49
Total	21 (100)	43 (100)	16 (100)	80

Layer 6 was split into three equal depths. The number of each cell type sampled within the depth is indicated. Percentages (in parentheses) show the proportion of each cell type relative to all cells at the same depth.

dendrite) did not project from the pial side of the soma. In fact these cells were essentially pyramidal cells that were rotated so that their “apical” dendrite ran, in most cases, parallel to the pia or, more rarely, into the white matter. The axons of these cells projected from the side of the soma opposite the “apical” dendrite. These cells were also found throughout the depth of layer 6 (Fig. 3A), and their counterparts in the rat somatosensory cortex had cortico-cortical projecting axons (Zhang and Deschenes 1997).

The great majority of cells (62/89, 69.7%), were “tufted” pyramidal cells (Fig. 2, *D* and *E*). These cells had a characteristic apical dendrite that had many near-perpendicular branches in layer 6, usually sparse perpendicular branches in layer 5B, and a tuft of dendritic branches that initiated in layer 5A and sometimes continued through layer 4. Their basal dendrites radiated in all directions but remained confined to layer 6. Among this group of cells, we found two morphologically distinct groups of cells, type I (which has a tuft in one layer, 5A) and type II (which has a tuft in two layers, 5A and 4).

Type I tufted neurons (Fig. 2*D*; 8/89, 9.0% of all cells) were found only in the lower third of layer 6 (Fig. 3A), and nearly the entire apical dendritic tuft was contained within layer 5A with no dendrites in layer 4. These cells were similar in both morphology and laminar depth to rat somatosensory cortex layer 6 cells that projected to both VPM and Po (Zhang and Deschenes 1997). Type II tufted neurons (Fig. 2*E*, 54/89, 60.7% of all cells) were found throughout layer 6 (Fig. 3A). They had a series of dendritic branches in layer 5A which continued into and branched in layer 4. Hence, a larger proportion of their apical dendritic tufts was in layer 4 compared with type I tufted cells. These cells were similar to rat somatosensory cortex layer 6 cells that projected only to VPM and not to Po (Zhang and Deschenes 1997). Our quantitative criterion for separating tufted cells into these two groups was the apical dendrite length in layer 4 divided by the sum of apical dendrite length in layer 4 plus layer 5A (“apical tuft ratio”). If this proportion was approximately zero, then the cell was classified as a type I tufted cell, whereas cells classified as type II tufted cells had a proportion >0.2 . In accordance to this classification system, the average tuft proportion of type I tufted cells (range: 0.00–0.05, mean = 0.008) was significantly different ($P < 0.0001$) from type II Tufted cells (range: 0.24–0.85, mean = 0.579; Fig. 3*B*).

We found a significant difference between type I and type II tufted cells in the depth of their somata within layer 6. We determined a normalized depth for each cell by dividing the distance from the cell body to the layer 6A/6B border by the thickness of layer 6A (0.0 = bottom of layer 6; 1.0 = top of

layer 6). The average depths for type I and type II neurons were 0.20 (range = 0.036–0.306) and 0.49 (range = 0.126–0.958), respectively. This difference was significant (Mann Whitney *U* Test, $P < 0.0005$). Because our sample was not uniformly distributed within the depth of layer 6, we divided layer 6 into three subregions based on depth to compare the proportion of type I and type II tufted cells in each portion (see Table 1). In the top and middle thirds of layer 6, the proportions of type II tufted cells did not differ (as a proportion of all layer 6 cells; 10/16, 62.5% in top third; 27/43, 62.8% in middle third). However, in the lower third of layer 6, the proportion of type II tufted cells was slightly lower to 57.1% (12/21). Type I tufted cells only resided in the lower third of the layer 6 and comprised more than a quarter of the population of cells from that portion of the layer (6/21, 28.6%). This nonuniform distribution explains why we sampled a relatively small number of type I tufted cells, however, even within the bottom third of layer 6, type II cells were twice as common as type I cells.

We were concerned that type I tufted and type II tufted cells could be part of the same continuum of cells. However, two pieces of evidence suggest that they are two distinct populations. When we plotted the depth ratio for the each cell against its respective apical tuft ratio, the cells fell into two separate groups suggesting that they are distinct (Fig. 3*B*). In addition, there was a difference between these two populations in the relationship between the cell depth and percentage of dendritic length in layer 5*B* (Fig. 3*C*). Type II cells showed a positive significant trend in this relationship such that as these cells got closer to layer 5*B* the percentage of their apical dendrite in layer 5*B* increased ($R^2 = 0.54$, $P < 0.0001$). Type I cells had the opposite trend; as cells got closer to layer 5*B* the percentage of their apical dendrite in layer 5*B* decreased ($R^2 = 0.44$). For cells in the bottom 31% of layer 6 (which contains all the type I tufted cells), there was a significant difference in the percentage of the apical dendrite in layer 5*B* between type I tufted cells (31.7%, range = 24.3–40.6%) and type II tufted cells (20.2%, range = 10.0–36.2%, Mann Whitney *U* Test, $P < 0.05$).

Previous studies have shown that cells in the rat somatosensory cortex have similar morphologies to what we have found in the rat visual cortex (Zhang and Deschenes 1997). More specifically, in the somatosensory cortex, cells in the lower half which project to VPM and Po also have an apical dendrite that has sparse branching in layer 5*B* and an apical tuft in layer 5*A*. Somatosensory cells in the upper half which project to VPM but not Po have an apical dendrite that tufts in layer 4. Based on these homologous relationships and earlier studies showing the sublaminar projections of the rat visual cortex (Bourassa and Deschenes 1995), we suspect that the type I tufted cells are projecting to LGN and LP, whereas type II tufted cells are only projecting to LGN.

A small group of layer 6 pyramidal cells (“non-tufted” cells, 5/89, 5.6%) were characterized by their long angular branches from the apical dendrite, especially at the layer 5*B*/6 border (Fig. 2*F*). Their apical dendrite did not end in a tuft, and these cells had homologous morphology to cortico-cortical projecting “short pyramidal” cells in rat somatosensory cortex. In addition, nontufted pyramidal cells were sampled only in the top half of layer 6 and with an average depth of 0.66 (range = 0.563–0.862), which was significantly different from type I tufted cells (Mann Whitney *U* Test, $P < 0.005$) and nearly

significantly different from type II tufted cells (Mann Whitney *U* Test, $P = 0.05$).

Photostimulation results

We used laser-scanning photostimulation to map the local sources of excitatory input to 59 layer 6 cells. A complete table of the photostimulation results for all of our cells is provided in Table 2 with sample local excitatory input patterns for each cell type provided in Figs. 4 and 6.

Type I and type II tufted cells had significant differences in their local laminar input (Figs. 4, *A* and *C*, and 5*A*). We collected photostimulation data for 7 type I tufted and 38 type II tufted pyramidal cells. Sample input patterns for type II and type I tufted pyramidal cells are shown in Fig. 4, *A* and *C*, respectively. All type I tufted and type II tufted cells received significant input from layer 6. Significant input from layer 5*B* was somewhat less common for type I tufted cells (5/7, 71.4%) than type II tufted cells (37/38, 97.4%; see Fig. 5*A*). This difference was nearly significant (Fisher’s exact test, $P = 0.06$). Significant input from layer 5*A* was significantly less common for type I tufted cells (1/7, 14.3%) than type II tufted cells (23/38, 60.5%; Fisher’s exact test, $P < 0.05$; Fig. 5*A*). Type I and type II tufted cells differed most significantly in their input from layer 4. Fifty-eight percent (22/38) of type II tufted cells received significant input from layer 4, whereas no type I tufted cell received significant input from layer 4 (Fisher’s exact test, $P < 0.01$; Fig. 5*A*). Neither cell type received much input from layer 2/3. Only two (2/38, 5.3%) type II tufted cells and no type I tufted cell received significant input from layer 2/3 (not significant; Fig. 5*A*).

We also analyzed the relative strength of excitatory input from each layer to the type I and type II tufted cells. Although these cells received differential inputs from superficial layers, the strongest inputs to both cell types came from layer 6 (Fig. 5*B*). Nevertheless, relative strength of input from the deeper layers differed between type I and type II tufted cells. Type I tufted cells received a greater percentage of their evoked excitatory input from layer 6 ($76.8 \pm 8.2\%$; mean \pm SE) than did type II tufted cells ($49.0 \pm 3.0\%$, Mann Whitney *U* test $P < 0.005$, Fig. 5*B*). Conversely, type II tufted cells received a larger percentage of their excitatory input from layer 5*B* ($36.1 \pm 2.4\%$) than did type I tufted cells ($20.4 \pm 6.4\%$, Mann Whitney *U* test $P < 0.05$, Fig. 5*B*).

As expected from the proportions of cells receiving significant layer 4 input, the relative strength of evoked input from layer 4 for type II tufted cells was significantly greater than for type I tufted cells (4.9 ± 1.1 vs. 0.0% , respectively, Mann Whitney *U* Test, $P < 0.05$, Fig. 5*B*). The relative strength of evoked input from layer 5*A* for type II tufted cells was greater than for type I tufted cells (9.9 ± 1.9 vs. $2.7 \pm 2.7\%$, respectively) but the difference was not significant (Mann Whitney *U* Test, $P = 0.08$, Fig. 5*B*).

Interneurons comprised seven cells of the population characterized with photostimulation. A typical excitatory input pattern to an interneuron is illustrated in Fig. 4*E*. All interneurons received significant input from both layers 5*B* and 6 (Fig. 5*A*). Only one inhibitory cell received significant input from layer 4 and layer 5*A* (1/7, 14.3%). However, five cells (5/7, 71.4%) received significant input from layer 2/3. The proportion of cells receiving input from layer 2/3 was significantly

TABLE 2. Laminar sources of evoked excitatory input for each cell

Cell Type	Cell Number	L2/3 Input, %	L4 Input, %	L5A Input, %	L5B Input, %	L6 Input, %
Non-Tuft	Z0416z	7.98	7.86	10.35	22.55	51.26
Non-Tuft	Z0331al	6.44	1.63	11.10	34.68	45.95
BIP	Z0124a	3.08	NS	11.83	55.34	29.75
BIP	Z0421z	NS	4.84	22.85	38.16	34.15
INV	Z0208a	NS	NS	6.54	25.62	67.64
INV	Z0902a	NS	NS	NS	17.52	82.48
INV	Z0203a	NS	NS	NS	NS	100.00
INT	Z1204c	3.51	13.88	12.10	43.90	28.61
INT	Z0903el	5.17	NS	NS	62.86	31.96
INT	Z0903b	2.54	NS	NS	26.05	71.41
INT	Z0826e	2.51	NS	NS	3.37	84.11
INT	Z0819al	0.62	NS	NS	48.05	51.33
INT	Z0203c	NS	NS	NS	22.95	77.05
INT	Z1204d	NS	NS	NS	70.07	29.93
Type I	Z0414d	NS	NS	19.16	42.16	38.58
Type I	Z0416c	NS	NS	NS	33.11	66.89
Type I	Z0417a	NS	NS	NS	30.34	69.68
Type I	Z0820a	NS	NS	NS	26.82	73.18
Type I	Z0423d	NS	NS	NS	10.53	89.47
Type I	Z0414a	NS	NS	NS	NS	100.00
Type I	Z0210b	NS	NS	NS	NS	100.00
Type II	Z1208c	2.28	1.11	9.20	18.77	68.64
Type II	Z0423al	1.60	5.39	10.87	59.81	22.74
Type II	Z1204e	NS	17.62	6.89	25.79	49.72
Type II	Z0414l	NS	15.03	2.34	42.39	40.24
Type II	Z0210al	NS	12.89	31.58	13.61	42.12
Type II	Z0407al	NS	11.63	20.67	46.51	21.19
Type II	Z0902c	NS	10.18	15.85	27.02	46.84
Type II	Z0418b	NS	8.18	19.63	33.47	38.71
Type II	Z0409b	NS	7.60	31.47	40.88	20.05
Type II	Z0423bl	NS	7.09	11.08	30.21	51.82
Type II	Z0409c	NS	5.07	14.62	54.03	26.28
Type II	Z0409dl	NS	4.48	5.30	50.21	40.01
Type II	D0408cl	NS	4.04	49.54	14.94	31.48
Type II	Z1217a	NS	2.19	23.05	32.75	42.01
Type II	Z0819b	NS	1.54	2.35	57.43	38.58
Type II	Z1209b	NS	0.94	11.87	33.79	53.40
Type II	Z1217b	NS	0.62	9.06	22.02	68.30
Type II	Z0407b	NS	28.54	NS	20.23	51.23
Type II	Z0826c	NS	17.02	NS	60.78	22.20
Type II	Z1217e	NS	12.66	NS	42.35	44.99
Type II	Z0407c	NS	6.56	NS	32.29	61.15
Type II	Z0414b	NS	4.78	NS	8.14	87.08
Type II	Z0414c	NS	NS	30.90	44.60	24.50
Type II	D0408bl	NS	NS	15.67	29.12	55.21
Type II	Z0819c	NS	NS	15.23	37.40	47.38
Type II	Z0414e	NS	NS	14.97	30.97	54.05
Type II	Z0826b	NS	NS	14.22	45.23	39.54
Type II	Z1208b	NS	NS	10.83	51.75	37.41
Type II	Z1209e	NS	NS	NS	56.58	43.42
Type II	Z0416d	NS	NS	NS	50.06	49.94
Type II	Z0903d	NS	NS	NS	50.02	49.98
Type II	Z0820b	NS	NS	NS	46.82	53.18
Type II	Z1208a	NS	NS	NS	42.27	57.73
Type II	Z0409a	NS	NS	NS	33.46	66.54
Type II	Z0902bl	NS	NS	NS	29.28	70.72
Type II	Z1217f	NS	NS	NS	28.47	71.53
Type II	Z0416a	NS	NS	NS	28.53	73.47
Type II	Z1209f	NS	NS	NS	NS	100.00

Cells are sorted by anatomical subtype. Layers with significant input to the cell show a percentage signifying the proportion of total evoked excitatory input that originated from that layer. Layers that provided nonsignificant input are denoted by NS. Values emboldened in the table correspond to cells shown in Figs. 2, 4, and 6. BIP, bipolar excitatory; INV, inverted pyramidal; INT, inhibitory interneurons.

greater than for each of the tufted pyramidal cell subtypes (Fisher exact test, type I, $P < 0.05$, type II, $P < 0.0005$, Fig. 5A). Nevertheless, the strongest excitatory input to layer 6 inhibitory cells was from the deeper layers, with $54.6 \pm 10.1\%$ of their input coming from layer 6 and $39.6 \pm 8.9\%$ of their input from layer 5B. Despite the prevalence of significant input from layer 2/3, it was quite weak; only $2.1 \pm 0.7\%$ of the excitatory input to interneurons came from layer 2/3. Nevertheless, the strength of input from layer 2/3 to interneurons was significantly more than it was to other cell types (Mann Whitney U test, $P < 0.005$). Also the strength of input from layer 5A was significantly less for interneurons than for type II tufted cells (Mann Whitney U test, $P < 0.05$).

Our photostimulation results for the other three cell types were limited. We only had photostimulation results for two nontufted cells, three bipolar excitatory cells, and three inverted pyramidal cells (see Table 2), which was not enough to draw a conclusion about possible differences between cell types. Sample input patterns for these three more rare subtypes are provided in Fig. 6. However, we did find that there was some internal consistency in these groups of cells. For example, both nontufted pyramidal cells received significant excitatory input from all the layers. Both bipolar excitatory cells received some significant superficial layer input and received stronger input from layer 5B than layer 6. All three inverted pyramidal cells received no significant superficial input and received their largest input from layer 6. Like other cell types, these cells all received the great majority of their excitatory inputs from layers 5B and 6 and not from more superficial layers.

In summary, our photostimulation results indicate that cells with different morphologies receive different patterns of laminar input. The most striking differences are between the two tufted pyramidal cell subtypes. Type I tufted cells have no detectable superficial excitatory input but receive strong excitatory input from the deeper layers, especially layer 6. Type II tufted cells also receive their strongest excitatory input from layer 6 but proportionally less than type I tufted cells. On the other hand, they receive stronger excitatory input from layers 4, 5A, and 5B. Finally, inhibitory interneurons and nontufted pyramids, which also receive their strongest excitatory input from layer 6, were the only cell subtypes that received significant excitatory input from layer 2/3.

DISCUSSION

Overview

Primary sensory cortices have many common organizational features across cortical areas and across species. For example, input from primary thalamic nuclei targets cortical layers 4 and 6, and corticothalamic feedback originates from layer 6 pyramidal neurons. Furthermore, the cortical layers containing neurons that project axons to layer 6 are also conserved across areas and species. These similarities suggest the layer 6 neurons might be connected similarly across cortical areas and play similar functional roles. Our findings, however, demonstrate that the sources of local excitatory input to layer 6 pyramidal neurons in the rat visual cortex are strikingly different from those in the monkey visual cortex. Monkey layer 6 pyramids can receive very strong input from superficial cortical

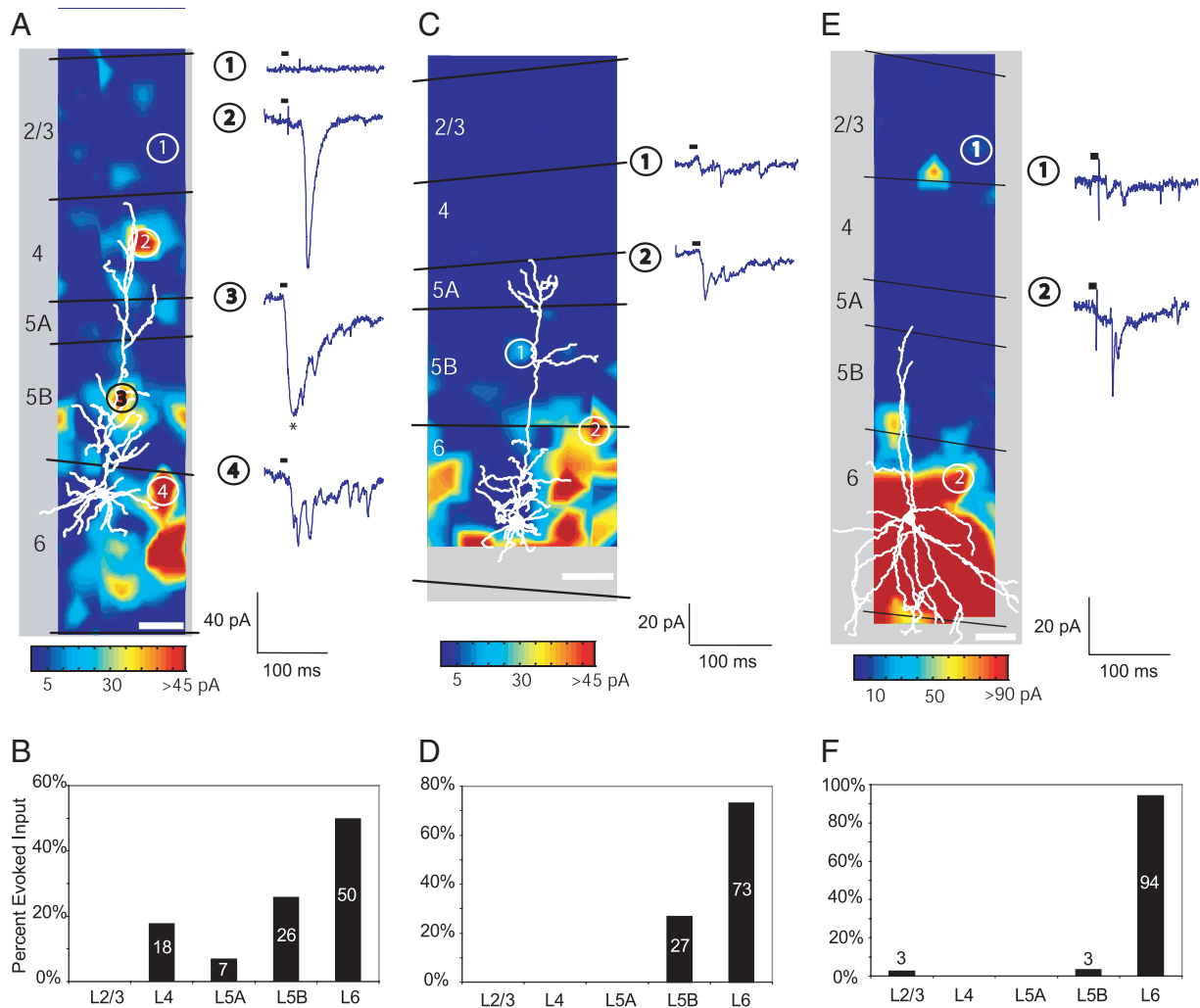


FIG. 4. Laminar excitatory input to 3 main types of layer 6 pyramidal cells. Pseudo-colored input maps demonstrate representative patterns of excitatory input to 3 individual neurons. These input maps are linear interpolations of the sum of excitatory postsynaptic current (EPSC) amplitude values (minus spontaneous EPSCs) measured after photostimulation at sites spaced $\sim 50 \mu\text{m}$ apart. Colored horizontal scale bars indicate the corresponding sum of EPSC amplitude values for input maps above. Camera lucida drawings of dendrites (white lines) and soma (white) are overlaid onto plots. Gray areas are present so that neuronal processes can be seen against otherwise white background. Laminar borders are represented by horizontal black lines and labeled on the left. To the right of each input map are example voltage-clamp recordings (-65 mV holding potential) made while stimulating presynaptic regions signified by the corresponding circled numbers. Short dashes above each trace show the duration of photostimulation and onset of glutamate activation. The current marked with an asterisk is a direct response to glutamate uncaging and was omitted from analysis. Percentage of evoked excitatory input (EI, see text) from each layer is illustrated in the bar graphs below each plot. **A**: type II tufted pyramidal neuron (*cell Z1204e*—see Table 2; Fig. 2D) that received significant input from layers 4, 5A, 5B, and 6, but not from layer 2/3. **B**: bar graph representing the percent of total evoked input from each layer for cell in **A**. In this case, the strongest input came from layer 6 followed by layer 5B. The weakest significant input came from layer 5A. **C**: type I tufted pyramidal neuron (*cell Z0423d*; Fig. 2E) that received significant input from layers 5B and 6, with no significant input from layers 2/3, 4, or 5A. **D**: bar graph representing the percent of total evoked input from each layer for cell in **C**. In this case, the strongest input came from layer 6 followed by layer 5B. **E**: inhibitory interneuron (*cell Z0826e*; Fig. 2A) that received significant input from layers 2/3, 5B, and 6, but no significant input from layers 4 or 5A. **F**: bar graph representing the percent of total evoked input from each layer for cell in **E**. In this case, the strongest input was from layer 6 with some weaker input from layer 2/3 and 5B. A brief electrical noise corresponding with shutter closure occurred in a few of these traces (i.e., trace 2 in **A**, trace 1 and 2 in **E**). White scale bars represent $200 \mu\text{m}$.

layers often exceeding the strength of deep layer input to the same cell (Briggs and Callaway 2001). In contrast, rat layer 6 neurons invariably received the great majority of their excitatory input from deep layers.

Previous anatomical studies of rat layer 6 cortical neurons identified a large diversity of morphological subtypes (van Brederode and Snyder 1992; Zhang and Deschenes 1997). Our study is no exception. In the rat visual cortex, we found six subtypes of neurons based on their dendritic morphology. Consistent with a different functional role for each layer 6 cell type, we also identify systematic differences in the laminar sources of local excitatory input to each cell type.

Cell-type-specific circuits

The most common types of pyramidal cells encountered in our study of the rat visual cortex are remarkably similar in their morphology to layer 6 pyramidal neurons in rat somatosensory cortex. Zhang and Deschenes (1997), who classified their cells based not only on dendritic morphology but also based on their axonal projections, found six subtypes of neurons, suggesting that these cells are common to sensory cortices and may play analogous functional roles. We have adopted the same names for our cell types when the homology was clear (i.e., excitatory bipolar cells, inverted

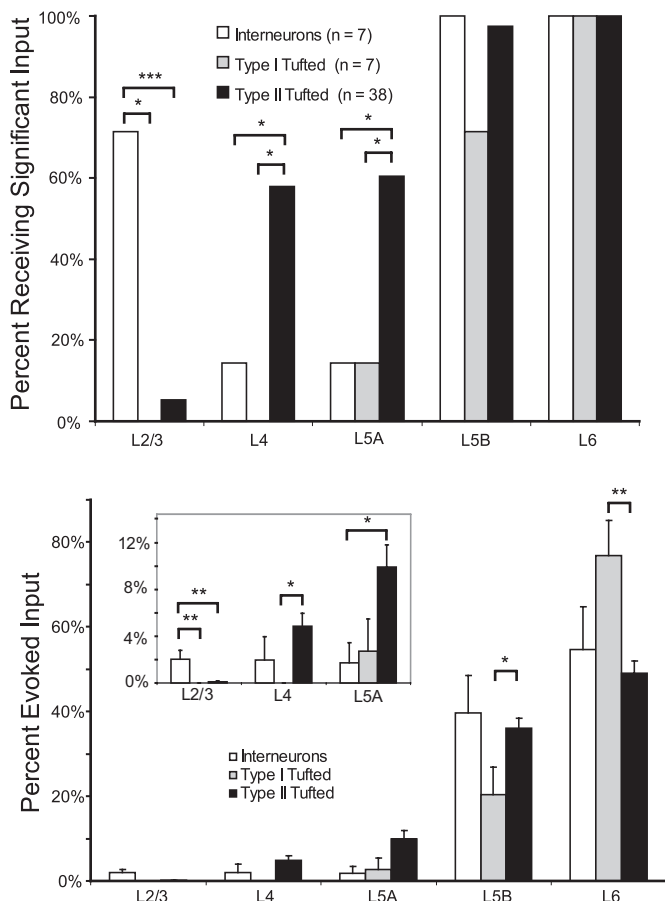


FIG. 5. Laminar input to the 3 main subtypes of layer 6 neurons. *A*: percentages of neurons of each type receiving significant input compared with spontaneous trials for each cortical layer. Interneurons as a group were more likely to receive significant input from layer 2/3 than other cell types (Fisher exact test, type I, $P < 0.05$, type II, $P < 0.0005$). Type II cells as a group received significantly more input from layer 4 (type I, $P < 0.01$, interneurons, $P < 0.05$) and layer 5A (type I, $P < 0.05$, interneurons, $P < 0.05$). Almost all cells received significant input from layer 5B. All cells, without exception received significant input from layer 6. *B*: mean \pm SE percentage of total evoked input for each layer for the 3 main subtypes of cells. *Inset*: enlargement of the input from the 3 superficial layers. Interneurons received a larger percentage of evoked input from layer 2/3 than other cell types (Mann Whitney U test, type I, $P < 0.005$, type II $P < 0.005$). Type II tufted cells received a larger percentage of their evoked input from layer 4 than did type I cells ($P < 0.05$) and from layer 5A than did interneurons ($P < 0.05$). Type II tufted cells also received a larger percentage of their evoked input from layer 5B compared with type I tufted cells ($P < 0.05$). Conversely, type I tufted cells received a larger percentage of their evoked input from layer 6 compared with type II tufted cells ($P < 0.005$). *, significance of $P < 0.05$; **, significance of $P < 0.005$; ***, significance of $P < 0.0005$.

pyramidal cells). One major change in terminology is our type I and type II tufted pyramidal cells, which we distinguished by dendritic morphology, whereas Zhang and Deschenes classified based on axonal projections. We find that the dendritic arbors of type I tufted cells are indistinguishable from the tufted cells in the somatosensory cortex that project to VPM and Po, whereas type II tufted cells are similar to those in the somatosensory cortex that project to VPM (Zhang and Deschenes 1997).

Furthermore, some subtypes of layer 6 cells have a sublaminal organization. Earlier studies of rat visual cortex found that cells in the upper and lower half had different thalamic projections (Bourassa and Deschenes 1995), a characteristic that is

also shared with the somatosensory cortex (Zhang and Deschenes 1997). Three main differences exist in the sublaminal organization of our cells and that of Zhang and Deschenes. First, they found cells homologous to our type II tufted cells in only the upper half of somatosensory cortex layer 6, whereas we found type II tufted cells throughout the layer. This discrepancy may be the result of a difference in classification criteria. Although Zhang and Deschenes found tufted pyramidal cells throughout the entire layer, they did not classify many of their cells because they could not identify their axonal projections. Hence it is unclear whether these cells would have met our criteria for Type II tufted cells. Second, Zhang and Deschenes found a much larger number of cells homologous to our nontufted pyramidal cells (23/84 vs. our 5/89) and did not find a sublaminal organization to these cells. This suggests that short pyramidal/nontufted cells may play a more common role in the rat somatosensory cortex than in visual cortex. Zhang and Deschenes found that some of the short pyramidal cells projected across the corpus callosum. In the visual cortex, cells projecting across the callosum are found close to the vertical meridian (Lund and Lund 1970) and are restricted to the top of layer 6 (as well as other layers) (Olavarría and Van Sluysers 1983). This difference could explain the small number and sublaminal organization of our nontufted cells. Finally, Zhang and Deschenes found a much larger number of cells homologous to our type I tufted cells, which they found in the lower half instead of lower third of layer 6.

In addition to our anatomical findings, we identified the laminar sources of functional excitatory input to individual neurons (see Fig. 7 for summary). Type I tufted cells received input mainly from layer 6 and layer 5B with none of the cells receiving significant input from the superficial layers. Type II tufted cells received input mainly from layer 6 and layer 5B but also, to a lesser extent, from layers 5A and 4. Furthermore, the proportion of layer 5B to layer 6 input was greater for type II tufted cells compared with type I tufted cells. Interneurons as a class received more input from layer 2/3 than any of the tufted groups. They also received significant input from layer 5B, but their strongest input was from layer 6.

Because the dendrites of layer 6 cells overlap with axonal projections of cells in all other layers, layer 6 cells potentially could have received input from any of the layers. The actual patterns of functional laminar input that we measured could not have been predicted from previous anatomical studies. It is clear from our study that cells in superficial layers connect to layer 6 cells with a high level of specificity. Several observations make this point. Although one might have predicted that type II tufted cells would receive more input from layer 4 than type I tufted cells because of their dendritic branches within that layer, one would not have predicted that the input from that layer would be so weak compared with the deeper layers. Based on morphology alone, one might predict that type I tufted cells would receive significant input from layer 5A and that the strength of this input would be greater than that for type II tufted cells. This is, of course, not the case because, as a class, type I tufted cells do not receive significant input from layer 5A and type II tufted cells receive stronger input from layer 5A than other cell types. Furthermore, because tufted cells have only short perpendicular dendritic branches in layer 5B, one might have predicted they would not get strong input from

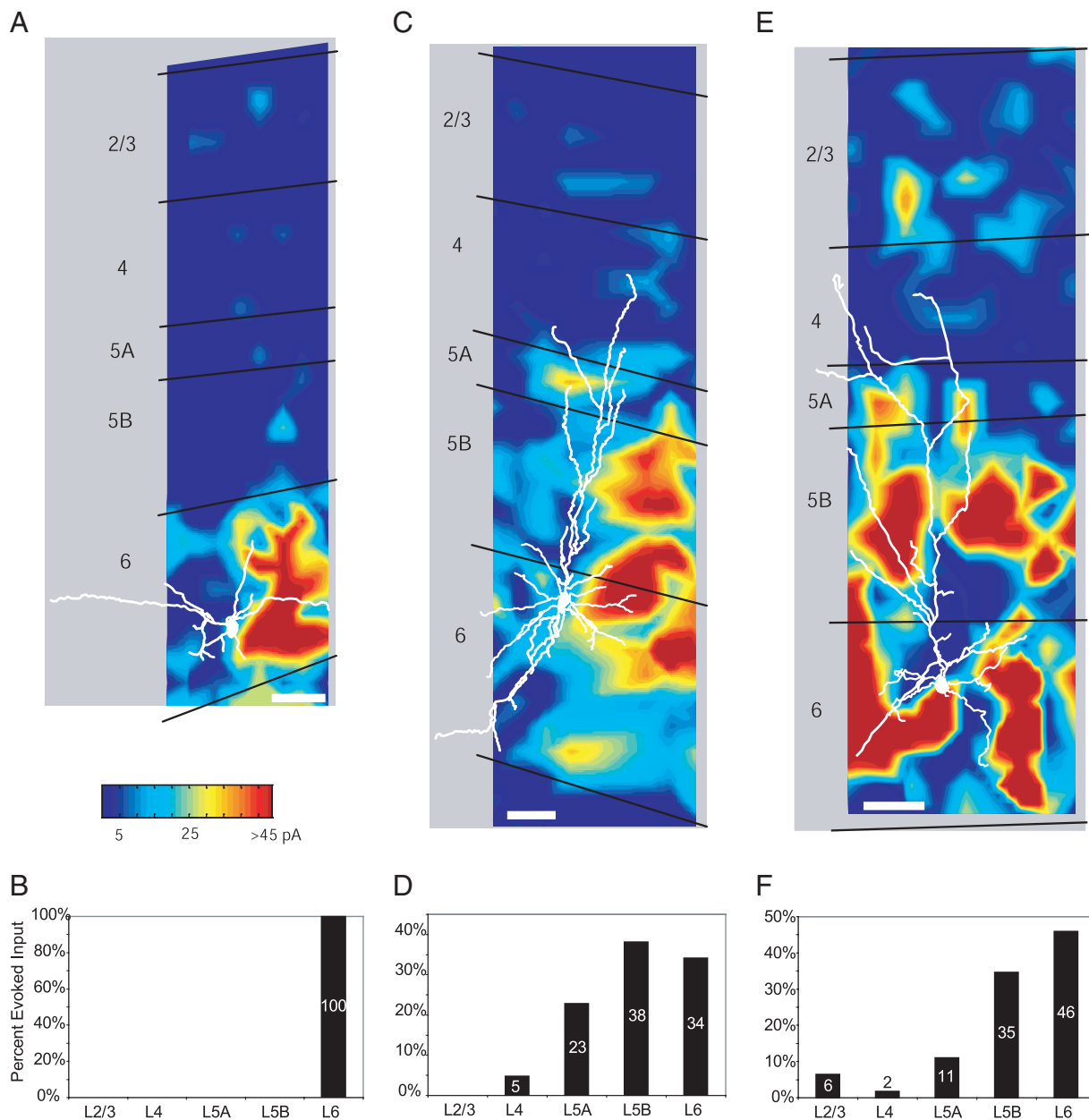


FIG. 6. Laminar excitatory input to 3 relatively rare subtypes of layer 6 pyramidal cells. Pseudo-colored input maps are similar to those described in Fig. 4. Colored horizontal scale bar in *A* applies to all 3 maps. *A*: inverted pyramidal neuron (cell Z0203a; Fig. 2C) that received significant input only from layer 6. *B*: bar graph representing the percent of total evoked input from each layer for cell in *A*. In this case, the only significant input came from layer 6. *C*: bipolar excitatory pyramidal neuron (cell Z0421z; Fig. 2B) that received significant input from layers 4, 5A, 5B, and 6 but not from layer 2/3. *D*: bar graph representing the percent of total evoked input from each layer for cell in *C*. In this case, the strongest input came from layer 5B followed closely by layer 6. The weakest significant input came from layer 4. *E*: nontufted pyramidal neuron (cell Z0331a1; Fig. 2F) that received significant input from all the layers. *F*: bar graph representing the percent of total evoked input from each layer for cell in *E*. In this case, the strongest input came from layer 6 followed by layer 5B. The weakest significant input came from layer 4. White scale bars represent 200 μm .

layer 5B. However, again, this was not the case; almost all the cells received significant strong input from layer 5B. From anatomical studies alone, it would not have been possible to predict that layer 2/3 connects preferentially with inhibitory interneurons, nor would it have been possible to predict that the strongest input to layer 6 cells is from other layer 6 cells.

Recent studies of paired recordings in layer 6 have suggested that cells that are morphologically similar to the Zhang and Deschenes cortico-cortical cells provide more of the excitatory

input to layer 6 pyramidal cells (Mercer et al. 2005), whereas those similar to corticothalamic cells provide excitatory input to interneurons (West et al. 2005). However, these studies used layer 6 cells from the cat visual cortex, the rat somatosensory cortex, and the rat visual cortex. It is unclear how many of the layer 6 pairs were specifically from rat visual cortex nor do they analyze the frequency of connections between cells of the same type (e.g., corticothalamic cells to corticothalamic cells). Hence, further work is necessary to test for the possibility of cell-type-specific connectivity within layer 6.

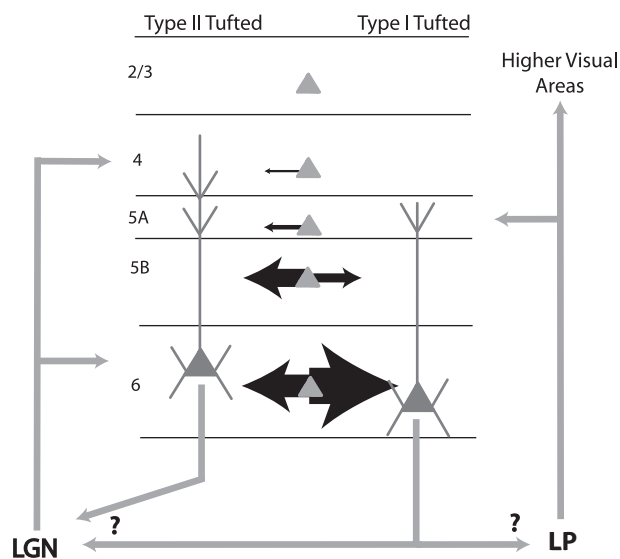


FIG. 7. Schematic diagram summarizing the functional input to 2 tufted types of pyramidal cells in layer 6. Thickness of black arrows represents the strength and directionality of the source of local excitatory input to the 2 different cell subtypes. Type II tufted cells receive significant local input from layers 4, 5A, 5B, and 6. The inputs from layers 4 and 5A are weak, whereas the inputs from layers 5B and 6 are strong and nearly equal to each other. Type I tufted cells only received significant local input from layers 5B and 6. The input from layer 6 is much larger than that from layer 5B. Based on previous work in the rat visual cortex and homology of these cells to those of the rat somatosensory cortex, Type II tufted cells probably project to LGN, whereas type I tufted cells project to both LGN and LP (middle gray arrows). Possible input to the layer 5A tufts of both cell types are projections from LP to layer 5A of rat visual cortex (gray arrows at right). Also, a possible input to the layer 4 tuft of type II tufted cells is thalamocortical axons from the LGN that terminate in layer 4 (gray arrows at left). Thalamocortical axons from the LGN also terminate in upper layer 6, likely connecting to both cell types. This data suggest that both cell types play a role in thalamocortical feedback loops, one involving LP and LGN (type I tufted cells), whereas the other is more close related to the LGN (type II tufted cells).

Species differences

Despite similarities in the basic organization and structure of cortex across areas and species, the rich overlap of axonal and dendritic arbors across all cortical layers provides for the possibility of connective diversity embedded within this common structure. Anatomical studies of cat visual cortex suggested that layer 5 was the main source of excitatory input to layer 6 and that the superficial layers did not provide strong input to this layer (see Gilbert 1983; Gilbert and Wiesel 1983). Because layer 5 does not receive direct geniculocortical input and the geniculocortical collaterals to layer 6 were sparser than those to layer 4, it was presumed that several stages of information processing preceded the flow of information to layer 6. In this model the thalamus drives layer 4, which in turn projects to layer 2/3, layer 2/3 to layer 5, and finally layer 6 is driven by layer 5. However, laser-scanning photostimulation studies in macaque primary visual cortex found that many layer 6 pyramidal neurons received strong functional input from more superficial layers, including layer 2/3 and layer 4, which could exceed the strength of input from layer 5 (Briggs and Callaway 2001). These findings supported a cortical circuitry model in which layer 6 plays an earlier and more integrative role in visual processing (Callaway 1998). It was unclear whether the differences in these two models reflected different methodology or if there were species differences.

In the present study, we used the same methods as Briggs and Callaway (2001) and find that in the rat, connections to layer 6 pyramidal neurons in visual cortex are strikingly different from those of monkeys. The connections in rat are, however, similar to those proposed for cat visual cortex (Gilbert 1983); local excitatory input arises predominantly from layers 5B and 6 with very little or no input from more superficial layers. These findings demonstrate major species differences between monkeys and rats in the connectivity of layer 6 pyramidal neurons in the visual cortex.

Monkey and rat visual cortices also differ in the relationships between layer 6 and higher-order thalamic nuclei. Layer 6 pyramids in macaque V1 do not project axons to the pulvinar (the higher-order thalamic nucleus homologous to LP) (Lund et al. 1975) and afferent axons from the pulvinar terminate in layer 2/3 of V1 rather than layer 5A (Ogren and Hendrickson 1977; Rezak and Benevento 1979), hence overlapping with only a small subset of layer 6 cells that project their apical dendrites to that layer. In contrast, layer 6 tufted pyramids in the rat visual cortex seem to play an important role in two corticothalamic systems. Type I tufted cells, which probably project to both LP and LGN, receive input only from layer 6 and layer 5B, the same two layers containing neurons that project to LP (Bourassa and Deschenes 1995). Furthermore, these cells have large, elaborate dendritic tufts in layer 5A, where they probably receive synaptic input from afferent axonal arbors of LP neurons (Herkenham 1980). Type II tufted cells, which probably project only to LGN, have dendritic tufts in layer 4 and a soma and basal dendrites in layer 6, the two layers that receive afferent axonal arbors from the LGN. Furthermore, they receive input from layer 4 and layer 6 cells, which are postsynaptic to geniculocortical pathway. In addition these cells also have dendritic tufts in layer 5A where they probably receive input from LP, and they receive strong input from layer 5B cells which project to LP. Hence, type II tufted cells probably provide the LGN with feedback reflecting activity in both corticothalamic systems. In the monkey, interactions with the pulvinar nucleus of the thalamus, instead involves only a population of layer 5 neurons that do not provide input to the LGN. Thus the two corticothalamic systems appear to operate more independently in the monkey visual system than in the rat.

These basic species differences in the circuitry of layer 6 cortical neurons might reflect more fundamental differences in the organization of the rodent versus the primate brain. One of the hallmarks of primate evolution is the remarkable enlargement of the cerebral cortex relative to subcortical brain structures (Clark et al. 2001; Finlay and Darlington 1995). These evolutionary changes are paralleled by similar increases in primates in the numbers of visual cortical areas and the numbers of neurons making direct cortico-cortical connections. Thus there has been a clear evolutionary trend for an increasing role of cortical relative to subcortical structures. Because connections from primary visual cortex to higher cortical areas originate from superficial cortical layers, the connection from superficial layers to layer 6 neurons in primate V1 may reflect the need to integrate this information with subcortical computations. In contrast, visually driven behaviors in rats are likely dominated by subcortical computations and therefore require less direct integration with superficial cortical layers. Alternatively, future studies investigating local input to layer 6 pyra-

midal neurons in the rat barrel cortex could reveal that superficial input is more closely related to the relative dominance of cortical versus subcortical processing systems in different sensory modalities rather than evolutionary trends.

ACKNOWLEDGMENTS

The authors thank D. J. Braiser for help in collecting a portion of the data.

GRANTS

This study was funded by National Institutes of Health Grants EY-10742 and MH-63912. A. Zarinpar was supported by Medical Scientist Training Program Grant NIGMS07198, Aginsky Endowment Fellowship, and Merck Fellowship.

REFERENCES

- Bourassa J and Deschenes M.** Corticothalamic projections from the primary visual cortex in rats: a single fiber study using biocytin as an anterograde tracer. *Neuroscience* 66: 253–263, 1995.
- Briggs F and Callaway EM.** Layer-specific input to distinct cell types in layer 6 of monkey primary visual cortex. *J Neurosci* 21: 3600–3608, 2001.
- Briggs F and Callaway EM.** Laminar patterns of local excitatory input to layer 5 neurons in macaque primary visual cortex. *Cereb Cortex* 15: 479–488, 2005.
- Callaway EM.** Local circuits in primary visual cortex of the macaque monkey. *Annu Rev Neurosci* 21: 47–74, 1998.
- Callaway EM and Katz LC.** Photostimulation using caged glutamate reveals functional circuitry in living brain slices. *Proc Natl Acad Sci USA* 90: 7661–7665, 1993.
- Clark DA, Mitra PP, and Wang SS.** Scalable architecture in mammalian brains. *Nature* 411: 189–193, 2001.
- Dantzker JL and Callaway EM.** Laminar sources of synaptic input to cortical inhibitory interneurons and pyramidal neurons. *Nat Neurosci* 3: 701–707, 2000.
- Finlay BL and Darlington RB.** Linked regularities in the development and evolution of mammalian brains. *Science* 268: 1578–1584, 1995.
- Gilbert CD.** Microcircuitry of the visual cortex. *Annu Rev Neurosci* 6: 217–247, 1983.
- Gilbert CD and Wiesel TN.** Functional organization of the visual cortex. *Prog Brain Res* 58: 209–218, 1983.
- Guillery RW and Sherman SM.** Thalamic relay functions and their role in corticocortical communication: generalizations from the visual system. *Neuron* 33: 163–175, 2002.
- Herkenham M.** Laminar organization of thalamic projections to the rat neocortex. *Science* 207: 532–535, 1980.
- Katz LC and Dalva MB.** Scanning laser photostimulation: a new approach for analyzing brain circuits. *J Neurosci Methods* 54: 205–218, 1994.
- Lund JS and Lund RD.** The termination of callosal fibers in the paravisceral cortex of the rat. *Brain Res* 17: 25–45, 1970.
- Lund JS, Lund RD, Hendrickson AE, Bunt AH, and Fuchs AF.** The origin of efferent pathways from the primary visual cortex, area 17, of the macaque monkey as shown by retrograde transport of horseradish peroxidase. *J Comp Neurol* 164: 287–303, 1975.
- Mercer A, West DC, Morris OT, Kirchhecker S, Kerkhoff JE, and Thomson AM.** Excitatory connections made by presynaptic cortico-cortical pyramidal cells in layer 6 of the neocortex. *Cereb Cortex*, 2005.
- Ogren MP and Hendrickson AE.** The distribution of pulvinar terminals in visual areas 17 and 18 of the monkey. *Brain Res* 137: 343–350, 1977.
- Olavarría J and Van Sluyters RC.** Widespread callosal connections in infragranular visual cortex of the rat. *Brain Res* 279: 233–237, 1983.
- Rezak M and Benevento LA.** A comparison of the organization of the projections of the dorsal lateral geniculate nucleus, the inferior pulvinar and adjacent lateral pulvinar to primary visual cortex (area 17) in the macaque monkey. *Brain Res* 167: 19–40, 1979.
- Sawatari A and Callaway EM.** Convergence of magno- and parvocellular pathways in layer 4B of macaque primary visual cortex. *Nature* 380: 442–446, 1996.
- Sawatari A and Callaway EM.** Diversity and cell type specificity of local excitatory connections to neurons in layer 3B of monkey primary visual cortex. *Neuron* 25: 459–471, 2000.
- Schubert D, Staiger JF, Cho N, Kotter R, Zilles K, and Luhmann HJ.** Layer-specific intracolumnar and transcolumar functional connectivity of layer V pyramidal cells in rat barrel cortex. *J Neurosci* 21: 3580–3592, 2001.
- van Brederode JF and Snyder GL.** A comparison of the electrophysiological properties of morphologically identified cells in layers 5B and 6 of the rat neocortex. *Neuroscience* 50: 315–337, 1992.
- West DC, Mercer A, Kirchhecker S, Morris OT, and Thomson AM.** Layer 6 Cortico-thalamic pyramidal cells preferentially innervate interneurons and generate facilitating EPSPs. *Cereb Cortex*, 2005.
- Yabuta NH and Callaway EM.** Cytochrome-oxidase blobs and intrinsic horizontal connections of layer 2/3 pyramidal neurons in primate V1. *Vis Neurosci* 15: 1007–1027, 1998a.
- Yabuta NH and Callaway EM.** Functional streams and local connections of layer 4C neurons in primary visual cortex of the macaque monkey. *J Neurosci* 18: 9489–9499, 1998b.
- Yoshimura Y, Dantzker JL, and Callaway EM.** Excitatory cortical neurons form fine-scale functional networks. *Nature* 433: 868–873, 2005.
- Zhang ZW and Deschenes M.** Intracortical axonal projections of lamina VI cells of the primary somatosensory cortex in the rat: a single-cell labeling study. *J Neurosci* 17: 6365–6379, 1997.
- Zhang ZW and Deschenes M.** Projections to layer VI of the posteromedial barrel field in the rat: a reappraisal of the role of corticothalamic pathways. *Cereb Cortex* 8: 428–436, 1998.